

Spectroscopy and Decay properties of the charmonium

Virendrasinh Kher^{1,2} Ajay Kumar Rai^{2*}

¹ Applied Physics Department, Polytechnic, The M.S. University of Baroda, Vadodara 390002, Gujarat, India

² Department of Applied Physics, Sardar Vallabhbhai National Institute of Technology, Surat 395007, Gujarat, India

Abstract: The mass spectra of charmonium are investigated using a Coulomb plus linear (Cornell) potential. Gaussian wave function in position space as well as in momentum space are employed to calculate the expectation value of potential and kinetic energy respectively. Various experimental states ($X(4660)(5^3S_1)$, $X(3872)(2^3P_1)$, $X(3900)(2^1P_1)$, $X(3915)(2^3P_0)$ and $X(4274)(3^3P_1)$ etc.) are assigned as charmonium states. We also study the Regge trajectories, pseudoscalar and vector decay constants, the Electric and Magnetic dipole transition rates and the annihilation decay width for charmonium states.

Key words: Potential Model, Mass spectrum, Decay constant, Regge trajectories.

PACS: 12.39.Jh, 12.40.Yx, 13.20.Gd, 13.20.Fc

1 Introduction

The discovery of the J/ψ , first bound state of c and \bar{c} quarks, known as charmonium, is published in Ref.[1], whereas Ref.[2] describes the first observation of the $\psi(2S)$ and marked the field of hadron spectroscopy with the beginning of an important testing ground for the properties of the strong interaction using QCD. Charmonium system allows the prediction of some of the parameters of the states, using non-relativistic and relativistic potential models, lattice QCD, NRQCD and sum rules [3]. Although the first charmonium state was discovered in 1974, there are still many puzzles in charmonium physics. The charmonium spectroscopy below the open charm threshold has been well measured and agrees with the theoretical expectations, however, there are still lack of adequate experimental **informations** and solid theoretical inductions for the charmonium states above the open charm threshold [4]. Recently many other new resonances named XYZ particles have been discovered and are still under examination as these states do not match the predictions of the non-relativistic or semi-relativistic $q\bar{q}$ potential models.

In 1976, Siegrist and others at MARK-I collaboration (SLAC) observed the resonance $\psi(4415)$ with mass 4415 ± 7 MeV [5]. In 1978, DASP collaboration observed **peaks** for $\psi(4040)$, $\psi(4160)$ and $\psi(4415)$ resonances with mass 4040 ± 10 , 4159 ± 20 and 4417 ± 10 MeV respectively using non-magnetic detector [6]. Ablikim and others at BES collaboration and Mo and others at Beijing Institute HEP, determined the resonance parameters for

$\psi(4040)$, $\psi(4160)$ and $\psi(4415)$ charmonium. Eichten identified that **these** three resonances are 3^3S_1 , 2^3D_1 and 4^3S_1 with linear plus Coulomb potential model [7] and most later potential model calculations **are agreed** with their identification. Recently, the LHCb collaboration measured the mass 4191^{+9}_{-8} MeV of the resonance $\psi(4160)$ with $J^{PC} = 1^{--}$ [8]. In the year 2007, a resonant structure was observed by Belle collaboration with mass $4664 \pm 11 \pm 5$ MeV [9] and after one year later same collaboration observed a clear peak in the $e^+e^- \rightarrow \Lambda_c^+ \Lambda_c^-$ invariant mass distribution and assumed that the observed peak to be a resonance **of** mass 4634^{+8}_{-8} MeV with the possibility of 5^3S_1 charmonium state [10].

Rapidis and others at SLAC, LGW collaboration, observed a resonance with mass 3772 ± 6 MeV, just above the threshold for the production of charmed particles [11]. In parallel observation, W. Bacino and others at SLAC discovered and confirmed the $\psi(3770)$ resonance with mass 3770 ± 6 MeV [12] and the parameters were determined by SLAC and LBL collaborations [13]. In 2006 BES Collaboration measured the precise measurements of the mass of $\psi(3770)$ resonance [14] and recently its parameters have been measured using the data collected with the KEDR detector [15]. The Belle collaboration reported the first observation of a new charmonium-like state with mass $3943 \pm 6 \pm 6$ MeV in the spectrum of masses recoiling from the J/ψ in the inclusive process $e^+e^- \rightarrow J/\psi + \text{anything}$, and denoted it as $X(3940)$ [16]. Later on, new measurement for the $X(3940)$ was performed by the same collaboration and the mass $3942^{+7}_{-6} \pm 6$

1) E-mail: vkhker@gmail.com

2) E-mail: raiajayk@gmail.com

MeV was reported [17]. The 3^1S_0 state can be a good candidate of the $X(3940)$ resonance [18, 19].

Evidence of a new narrow resonance $X(3823)$ was found by Belle [20], with its mass near to potential model expectations for the centroid of the 1^3D_J states. Recently, BESIII Collaboration [21], observed a narrow resonance $X(3823)$ through the process $e^+e^- \rightarrow \pi^+\pi^-X(3823)$ and confirmed that it is a good candidate for the $\psi(1^3D_2)$ charmonium state.

In year 2003, Belle Collaboration observed charmonium like state in the decay process $B^\pm \rightarrow K^\pm\pi^+\pi^-J/\psi$ with mass $3872 \pm 0.6 \pm 0.5$ MeV [22] and was confirmed by CDF, D0 and BABAR Collaboration experiments [23–25]. Several properties of the $X(3872)$ have been determined [26–28] and CDF collaboration explained the $X(3872)$ particle as a conventional charmonium $c\bar{c}$ state with J^{PC} be either 1^{++} or 2^{-+} [29]. Recently BES III collaboration reported the first observation of process $e^-e^- \rightarrow \gamma X(3872)$ with mass $3871 \pm 0.7 \pm 0.2$ MeV [30]. Barnes and Godfrey in 2003, evaluated the strong and electromagnetic decays and considered all possible 1D and 2P charmonium assignments for $X(3872)$ [31].

The $X(3915)$ was observed by S.K.Choi and his team at Belle Collaborations [32] and later on BABAR collaboration confirmed the existence of the charmonium-like resonance $X(3915)$ and measured its mass $3919.4 \pm 2.2 \pm 1.6$ MeV with the $J^{PC} = 0^{++}$ option [33, 34]. This state is conventionally identified as the $\chi_{c0}(2P)$ charmonium [35, 36]. The Belle Collaboration in the year 2005, observed the $Z(3930)$ resonance in the $\gamma\gamma \rightarrow D\bar{D}$ process [37] with mass $3929 \pm 5 \pm 2$ MeV and considered it as a strong candidate for the $\chi_{c2}(2P)$ state. **BABAR Collaboration was confirmed the $Z(3930)$ resonance as the $\chi_{c2}(2P)$ state with mass $3926.7 \pm 2.7 \pm 1.1$ MeV and quantum numbers $J^{PC} = 2^{++}$ [38].**

In the year 2013, the BESIII collaboration observed a new structure with mass $3899 \pm 3.6 \pm 4.9$ MeV in the $\pi^\pm J/\psi$ mass spectrum (referred as $Z_c(3900)$) [39] and simultaneously Belle collaboration also observed a structure with mass $3894.5 \pm 6.6 \pm 4.5$ MeV in the $\pi^\pm J/\psi$ mass spectrum [40]. Observations of Xiao and his team, based on e^+e^- annihilations at $\sqrt{s} = 4170$ MeV, provide independent confirmation of the existence of the $Z_c^\pm(3900)$ state and provide new evidence for the existence of the neutral member $Z_c^0(3900)$ [41]. Recently BES III Collaboration performed an analysis **with favor to** the assignment of the $J^P = 1^+$ quantum numbers [42].

In year 2009, CDF collaboration reported evidence for a narrow structure near $J/\psi\phi$ threshold in $B^+ \rightarrow J/\psi\phi K^+$ decays with mass $4143 \pm 2.9 \pm 1.2$ MeV [43] and recently observed by the CMS [44] and D0 [45, 46] collaborations. It has been suggested that the $X(4140)$ resonance could be a molecular state [47–50], a tetraquark state [51–53] or a hybrid state [54, 55]. Searches

for the narrow $X(4140)$ were negative in LHCb [56] and BaBar [57] experiments. In 2011, the CDF Collaboration observed the $X(4140)$ structure with a statistical significance greater than 5 standard deviations and also find evidence for a second structure $X(4274)$ with a mass of $4274.4_{-6.7}^{+8.4} \pm 1.9$ MeV [58]. Very recently the LHCb Collaboration confirmed the resonance $X(4140)$ with mass $4146.5 \pm 4.5_{-2.8}^{+4.6}$ MeV and $X(4274)$ with mass $4273.3 \pm 8_{-3.6}^{+17.2}$ MeV in the $J/\psi\phi$ invariant mass distribution and determined their spin-parity quantum numbers to be $J^{PC} = 1^{++}$ for both [59]. They also investigated two new structures named as the $X(4500)$ and $X(4700)$ in the high $J/\psi\phi$ mass region. Ref.[60] suggest that $X(4274)$ can be a good candidate for the conventional $\chi_{c1}(3^3P_1)$ state. Study of charmonium in relativistic Dirac formalism with linear confinement potential indicate that the $X(4140)$ state can be admixture of two P states whereas $X(4630)$ and $X(4660)$ are the admixed of S-D wave state[61].

Recently developed (GSPM) generalized screened potential model [62], the non-relativistic, Coulomb gauge QCD approach [63], the light front quark model(LFQM) [64], the relativistic quark model [65], the effective field theory framework of potential non-relativistic QCD (pNRQCD) approach [66], the effective Lagrangian approach [67], lattice QCD [68, 69], LCQCD and QCD sum rules [70, 71] and the widely used potential models [72–78], are different theoretical model have been employed in theory to study the charmonium spectrum. The Cornell potential model is well known among the many phenomenologically successful potential models, which describes the charmonium system quite well.

The recent experimental results on new charmonium-like XYZ states indicate that they can be interpreted as above threshold charmonium levels and cannot be assigned to any charmonium states in the conventional quark model. These experimental results, motivate us and renewed theoretical interest to carry out a spectroscopic study and decay properties of charmonium.

In this article, to calculate the mass spectrum of the charmonium, we use Gaussian wave function both in position space as well as momentum space with a potential model, incorporating corrections to the kinetic energy of quarks as well as incorporating the relativistic correction of $\mathcal{O}(\frac{1}{m})$ to the potential energy part of the Hamiltonian. We also investigate the Regge trajectories in both the $(M^2 \rightarrow J)$ and $(M^2 \rightarrow n)$ planes (where J is the spin and n is the principal quantum number) using our predicted masses for the charmonium, as the Regge trajectories play a significant role to identify the nature of current and future experimentally observed charmonium states. We also obtained the pseudoscalar and vector decay constants for charmonium as well as the radiative (Electric and Magnetic dipole) transition rates and the

annihilation decay.

The article is organized as follows. Section 2.1, present the theoretical framework for the mass spectra, Section 2.2 present the decay constants ($f_{P/V}$), Section 2.3 present the radiative (E1 and M1) transitions in and Section 2.4 present annihilation decays. In Section 3, we discuss results for the mass spectra, ($f_{P/V}$) decays, E1 and M1 transition width as well as annihilation decays. The Regge trajectories from estimated masses in the (J, M^2) and (n_r, M^2) planes are in Section 3.1. Finally, we draw our conclusion in Section-4.

2 Methodology

2.1 Cornell potential with $\mathcal{O}(\frac{1}{m})$ corrections

Inspired by the extensive progress made in the experimental observation as well as the theoretical development of the charmonium, here we calculate the mass spectra and decay properties the charmonium within the widely used coulomb plus linear potential, Cornell potential [72, 73, 79, 80]. In this approach, we consider the relative corrections to the kinetic energy part and $\mathcal{O}(\frac{1}{m})$ correction to the potential energy part [81–83], which is inspired from the pNRQCD (potential non-relativistic quantum chromodynamics) [3, 84, 85]. The Cornell potential working well for heavy light flavour, hence we employed it for heavy-heavy flavour.

We employ following Hamiltonian [82, 83, 86, 87] and quark-antiquark potential [81] to study of the charmonium mass spectroscopy,

$$H = \sqrt{\mathbf{p}^2 + m_Q^2} + \sqrt{\mathbf{p}^2 + m_{\bar{Q}}^2} + V(\mathbf{r}), \quad (1)$$

$$V(r) = V^{(0)}(r) + \left(\frac{1}{m_Q} + \frac{1}{m_{\bar{Q}}}\right) V^{(1)}(r) + \mathcal{O}\left(\frac{1}{m^2}\right). \quad (2)$$

Here, $m_Q(m_{\bar{Q}})$ is the quark(anti-quark) mass. and The Cornell-like potential $V^{(0)}$ [78] and leading order perturbation theory yields $V^{(1)}(r)$ are,

$$V^{(0)}(r) = -\frac{4\alpha_S(M^2)}{3r} + Ar + V_0 \quad (3)$$

$$V^{(1)}(r) = -C_F C_A \alpha_s^2 / 4r^2 \quad (4)$$

where $\alpha_S(M^2)$, A , V_0 and $C_F = 4/3$, $C_A = 3$ is the strong running coupling constant, potential parameter, potential constant and the Casimir charges respectively. **This correction was original studied by Y.Koma, where the relativistic correction to the QCD static potential $\mathcal{O}(\frac{1}{m})$ was investigated non-perturbatively. This correction is found to be similar to the Coulombic term of the static potential when applied to charmonium. The leading order corrections are classified in powers of the inverse of heavy quark mass[81].**

Here, to estimate the expected values of the Hamiltonian with the Ritz variational strategy, we use Gaussian wave function in position space **as well as** in momentum space [82, 83] has the form

$$R_{nl}(\mu, r) = \mu^{3/2} \left(\frac{2(n-1)!}{\Gamma(n+l+1/2)} \right)^{1/2} (\mu r)^l \times e^{-\mu^2 r^2 / 2} L_{n-1}^{l+1/2}(\mu^2 r^2) \quad (5)$$

and

$$R_{nl}(\mu, p) = \frac{(-1)^n}{\mu^{3/2}} \left(\frac{2(n-1)!}{\Gamma(n+l+1/2)} \right)^{1/2} \left(\frac{p}{\mu} \right)^l \times e^{-p^2 / 2\mu^2} L_{n-1}^{l+1/2} \left(\frac{p^2}{\mu^2} \right) \quad (6)$$

respectively with the Laguerre polynomial L and the variational parameter μ . We estimated μ for each state, for the prefer value of A , using [87],

$$\langle K.E. \rangle = \frac{1}{2} \left\langle \frac{rdV}{dr} \right\rangle \quad (7)$$

To integrate relativistic correction, we enlarge Hamiltonian Eq.(1) with powers up to $\mathcal{O}(\mathbf{p}^{10})$ and $\mathcal{O}(\frac{1}{m})$ at the kinetic energy and the potential energy part respectively [82]. **We use a position space Gaussian wave-function to obtain expected value of the potential energy part whereas for the kinetic energy part, we use a momentum space wave-function using virial theorem Eq.(7).**

We adapted the ground state center of weight mass and equated with the PDG data by fixing A , α_s and V_0 using the following equation [88, 89]:

$$M_{SA} = M_P + \frac{3}{4}(M_V - M_P), \quad (8)$$

We also forecast the center of weight mass for the nJ state as [88]:

$$M_{CW,n} = \frac{\Sigma_J(2J+1)M_{nJ}}{\Sigma_J(2J+1)} \quad (9)$$

In the case of quarkonia, bound states are represented by $n^{2S+1}L_J$, identified with the J^{PC} values, with $\vec{J} = \vec{L} + \vec{S}$, $\vec{S} = \vec{S}_Q + \vec{S}_{\bar{Q}}$, parity $P = (-1)^{L+1}$ and the charge conjugation $C = (-1)^{L+S}$ with (n, L) being the radial quantum numbers. The spin dependent interaction are required to remove the degeneracy of charmonium states and can be written as [73, 90–92].

$$V_{SD} = V_{LS}(r) (\vec{L} \cdot \vec{S}) + V_{SS}(r) \left[S(S+1) - \frac{3}{2} \right] + V_T(r) \left[S(S+1) - \frac{3(\vec{S} \cdot \vec{r})(\vec{S} \cdot \vec{r})}{r^2} \right] \quad (10)$$

where the spin-spin, the spin-orbit and the tensor interactions can be written in terms of the vector and scalar parts of the $V(r)$ as by [91]

$$V_{SS}(r) = \frac{1}{3m_Q^2} \nabla^2 V_V = \frac{16\pi\alpha_s}{9m_Q^2} \delta^3(\vec{r}), \quad (11)$$

$$V_{LS}(r) = \frac{1}{2m_Q^2 r} \left(3 \frac{dV_V}{dr} - \frac{dV_S}{dr} \right), \quad (12)$$

$$V_T(r) = \frac{1}{6m_Q^2} \left(3 \frac{d^2 V_V}{dr^2} - \frac{1}{r} \frac{dV_V}{dr} \right), \quad (13)$$

where $V_V (= -\frac{4\alpha_s}{3r})$ is the coulomb part and $V_S (= Ar)$ is the confining part of Eq.(3)

In the present study, the quark masses is $m_c = 1.55$ GeV to reproduce the ground state masses of the charmonium. The fitted potential parameters are $A = 0.160$ GeV², $\alpha_s = 0.333$ and $V_0 = -0.23074$ GeV.

2.2 Decay Constants ($f_{P/V}$)

The decay constants with the QCD correction factor are computed using the Van-Royen-Weisskopf formula [93, 94],

$$f_{P/V}^2 = \frac{12 |\psi_{P/V}(0)|^2}{M_{P/V}} \left(1 - \frac{\alpha_s}{\pi} \left[2 - \frac{m_Q - m_{\bar{q}}}{m_Q + m_{\bar{q}}} \ln \frac{m_Q}{m_{\bar{q}}} \right] \right); \quad (14)$$

The Eq.(14) also gives the inequality[95]

$$\sqrt{m_v} f_v \geq \sqrt{m_p} f_p \quad (15)$$

Our results are in accordance with Eq.(15) and tabulated in Table(1). The value in parenthesis is the decay constant with QCD correction.

2.3 Radiative Transitions

The radiative transition is influenced by the matrix element of the EM current between the initial i and final f quarkonium state, i.e., $\langle f | j_{em}^\mu | i \rangle$. The electric dipole ($E1$) or magnetic dipole ($M1$) transition are leading order transition amplitudes [96–98].

The $E1$ matrix elements are estimated by[99]

$$\Gamma_{(E1)} \left(n^{2S+1} L_J \rightarrow n'^{2S'+1} L'_{J'} + \gamma \right) = \frac{4\alpha e_Q^2 E_\gamma^3 E_f}{3 M_i} C_{fi} \delta_{SS'} \times |\langle f | r | i \rangle|^2 \quad (16)$$

where Photon energy $E_\gamma = \frac{M_i^2 - M_f^2}{2M_i^2}$; the fine structure constant $\alpha = 1/137$; the quark charge e_Q in units of the electron charge and the energy of final state E_f . The angular momentum matrix element C_{fi} is

$$C_{fi} = \max(L, L') (2J' + 1) \begin{Bmatrix} L' & J' & S \\ J & L & 1 \end{Bmatrix}^2 \quad (17)$$

where $\{:::\}$ is a 6-j symbol. The matrix elements $\langle n'^{2S'+1} L'_{J'} | r | n^{2S+1} L_J \rangle$ were evaluated using the wavefunctions

$$\langle f | r | i \rangle = \int dr R_{n_i l_i}(r) R_{n_f l_f}(R) \quad (18)$$

The $M1$ radiative transitions are evaluated **using** the following expression [73, 100]

$$\Gamma_{M1} \left(n^{2S+1} L_J \rightarrow n'^{2S'+1} L'_{J'} \right) = \frac{4\alpha e_Q^2 E_\gamma^3 E_f}{3m_Q^2 M_i} S_{fi} |\mathcal{M}_{fi}|^2, \quad (19)$$

where,

$$\mathcal{M}_{fi} = \int dr R_{n_i l_i}(r) j_0(E_\gamma r/2) R_{n_f l_f}(R) \quad (20)$$

and

$$S_{fi} = 6(2S+1)(2S'+1)(2J'+1) \times \begin{Bmatrix} J & 1 & J' \\ S' & L & S \end{Bmatrix}^2 \begin{Bmatrix} 1 & 1/2 & 1/2 \\ 1/2 & S' & S \end{Bmatrix}^2 \quad (21)$$

here $L = 0$ for S-waves and $j_0(x)$ is the spherical Bessel function.

The $E1$ and $M1$ radiative transition widths are listed in table (5) and (6) respectively.

2.4 Annihilation Decays

Decays of quarkonia states into leptons or photons or gluons is extremely useful for the production and identification of resonances as well as the leptonic decay rates of quarkonia. It can also assist to recognize conventional mesons and multi-quark structures [101, 102].

2.4.1 Leptonic decays

The 3S_1 and 3D_1 states have $J^{PC} = 1^{--}$ quantum numbers, annihilate into lepton pairs through a single virtual photon. The leptonic decay width of the (3S_1) and (3D_1) states of charmonium including first order radiative QCD correction is given by [100, 101, 103].

$$\Gamma(n^3S_1 \rightarrow e^+e^-) = \frac{4e_Q^4 \alpha^2 |R_{nS}(0)|^2}{M_{nS}^2} \left(1 - \frac{16\alpha_s}{3\pi} \right) \quad (22)$$

$$\Gamma(n^3D_1 \rightarrow e^+e^-) = \frac{25e_Q^2 \alpha^2 |R''_{nD}(0)|^2}{2m_Q^4 M_{nD}^2} \left(1 - \frac{16\alpha_s}{3\pi} \right) \quad (23)$$

where, M_{nS} is mass of the decaying charmonium state.

Table 1. Pseudoscalar and vector decay constants (in GeV).

Decay	State	Our Work	Expt.[4]	[105]	[106]	[61]
f_P	1S	0.501(0.395)	0.335 ± 0.075	0.471(0.360)	0.404	
	2S	0.301(0.237)		0.344(0.286)	0.331	
	3S	0.264(0.208)		0.332(0.254)	0.291	
	4S	0.245(0.193)		0.312(0.239)		
	5S	0.233(0.184)				
	6S	0.224(0.177)				
f_V	1S	0.510(0.402)	0.411 ± 0.005	0.462(0.317)	0.375	0.420
	2S	0.303(0.239)	0.271 ± 0.008	0.369(0.253)	0.295	0.285
	3S	0.265(0.209)	0.174 ± 0.018	0.329(0.226)	0.261	0.218
	4S	0.240(0.194)		0.310(0.212)	0.240	0.166
	5S	0.234(0.185)		0.290(0.199)		0.106
	6S	0.225(0.177)				

2.4.2 Decay into photons

The annihilation decay of the charmonium states into two or three photon, without and/or with radiative QCD corrections are given by[100, 101]

$$\Gamma(n^1S_0 \rightarrow \gamma\gamma) = \frac{3e_Q^4 \alpha^2 |R_{nS}(0)|^2}{m_Q^2} \left(1 - \frac{3.4\alpha_s}{\pi}\right) \quad (24)$$

$$\Gamma(n^3P_0 \rightarrow \gamma\gamma) = \frac{27e_Q^4 \alpha^2 |R'_{nP}(0)|^2}{m_Q^4} \left(1 + \frac{0.2\alpha_s}{\pi}\right) \quad (25)$$

$$\Gamma(n^3P_2 \rightarrow \gamma\gamma) = \frac{36e_Q^4 \alpha^2 |R'_{nP}(0)|^2}{5m_Q^4} \left(1 - \frac{16\alpha_s}{3\pi}\right) \quad (26)$$

$$\Gamma(n^3S_1 \rightarrow 3\gamma) = \frac{4(\pi^2 - 9)e_Q^6 \alpha^3 |R_{nS}(0)|^2}{3\pi m_Q^2} \times \left(1 - \frac{12.6\alpha_s}{\pi}\right) \quad (27)$$

2.4.3 Decay into gluons

The annihilation decay of the charmonium states into two or three gluon as well as into gluons with photon and light quark, without and/or with radiative QCD correction are given by[100–102, 104]

$$\Gamma(n^1S_0 \rightarrow gg) = \frac{2\alpha_s^2 |R_{nS}(0)|^2}{3m_Q^2} \left(1 + \frac{4.8\alpha_s}{\pi}\right) \quad (28)$$

$$\Gamma(n^3P_0 \rightarrow gg) = \frac{6\alpha_s^2 |R'_{nP}(0)|^2}{m_Q^4} \quad (29)$$

$$\Gamma(n^3P_2 \rightarrow gg) = \frac{8\alpha_s^2 |R'_{nP}(0)|^2}{5m_Q^4} \quad (30)$$

$$\Gamma(n^1D_2 \rightarrow gg) = \frac{2\alpha_s^2 |R''_{nD}(0)|^2}{3\pi m_Q^6} \quad (31)$$

$$\Gamma(n^3S_1 \rightarrow 3g) = \frac{10(\pi^2 - 9)\alpha_s^3 |R_{nS}(0)|^2}{81\pi m_Q^2} \times \left(1 - \frac{3.7\alpha_s}{\pi}\right) \quad (32)$$

$$\Gamma(n^1P_1 \rightarrow 3g) = \frac{20\alpha_s^3 |R'_{nP}(0)|^2}{9\pi m_Q^4} \ln(m_Q \langle r \rangle) \quad (33)$$

$$\Gamma(n^3D_1 \rightarrow 3g) = \frac{760\alpha_s^3 |R''_{nD}(0)|^2}{81\pi m_Q^6} \ln(4m_Q \langle r \rangle) \quad (34)$$

$$\Gamma(n^3D_2 \rightarrow 3g) = \frac{10\alpha_s^3 |R''_{nD}(0)|^2}{9\pi m_Q^4} \ln(4m_Q \langle r \rangle) \quad (35)$$

$$\Gamma(n^3D_3 \rightarrow 3g) = \frac{40\alpha_s^3 |R'_{nP}(0)|^2}{9\pi m_Q^6} \ln(4m_Q \langle r \rangle) \quad (36)$$

$$\Gamma(n^3S_1 \rightarrow \gamma gg) = \frac{8(\pi^2 - 9)e_Q^2 \alpha \alpha_s^2 |R_{nS}(0)|^2}{9\pi m_Q^2} \times \left(1 - \frac{6.7\alpha_s}{\pi}\right) \quad (37)$$

$$\Gamma(n^3P_1 \rightarrow q\bar{q} + g) = \frac{8\eta_f \alpha_s^3 |R'_{nP}(0)|^2}{9\pi m_Q^4} \ln(m_Q \langle r \rangle) \quad (38)$$

The calculated annihilation decay width of charmonium are listed in Tables(7 to 13).

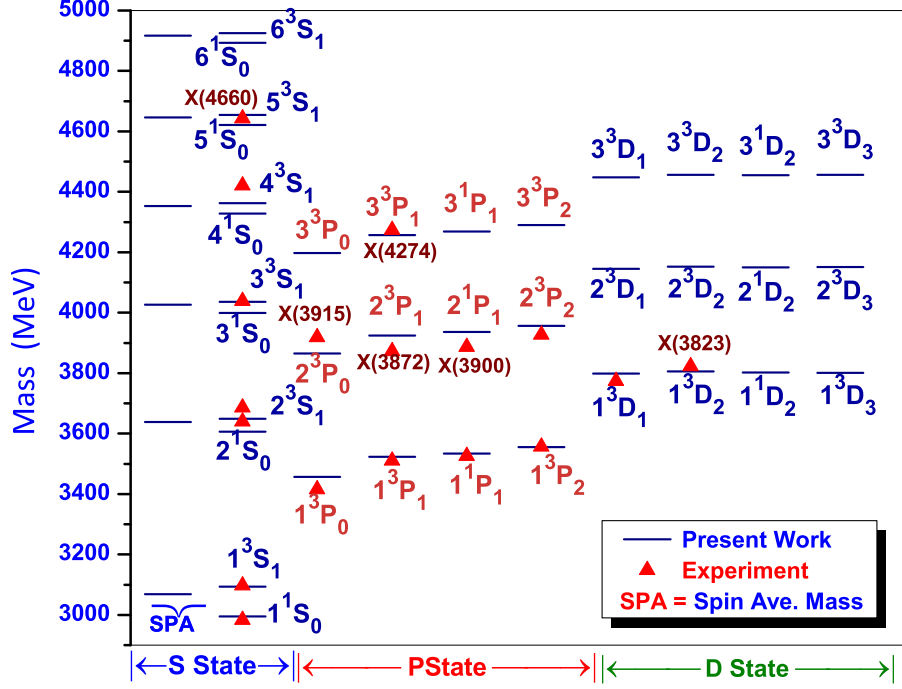


Fig. 1. Mass spectrum.

Table 2. S-P-D-wave center of weight masses (in GeV). (LP = Linear potential model, SP = Screened potential model, NR = Non-relativistic and RE = Relativistic)

nL	This work			Others Theory M_{SA} in (GeV)									
	μ (GeV)	M_{SA} (GeV)	Expt.[4] (GeV)	LP (SP) [79]	[107]	[108]	[76]	NR (GI)[73]	[75]	[109]	[110]	RE(NR)[111]	[112]
1S	0.716	3.068	3.068	3.068 (3.069)	3.090	3.067	3.061	3.063 (3.067)	3.068	3.068	3.068	3.068 (3.063)	3.068
2S	0.469	3.638	3.674	3.668 (3.668)	3.667	3.673	3.676	3.662 (3.663)	3.661	3.664	3.662	3.657 (3.661)	3.665
3S	0.412	4.027		4.071 (4.024)	4.070	4.027	4.080	4.065 (4.091)	4.014	4.075	4.064	4.051 (4.064)	4.090
4S	0.382	4.353		4.406 (4.277)	4.408	4.421	4.406	4.400 (4.444)	4.267			4.350 (4.400)	
5S	0.363	4.646		4.706 (4.469)	4.710	4.831			4.459			4.655 (4.694)	
6S	0.349	4.917			4.987	5.164			4.603			4.907 (4.973)	
1P	0.484	3.534	3.525	3.524 (3.527)	3.523	3.525	3.525	3.522 (3.523)	3.524	3.526	3.526	3.554 (3.519)	3.523
2P	0.416	3.936		3.945 (3.919)	3.941	3.926	3.945	3.942 (3.961)	3.913	3.960	3.945	3.963 (3.938)	3.962
3P	0.384	4.269		4.291 (4.238)	4.289	4.337	4.316	4.286 (4.323)	4.188			4.296 (4.283)	
1D	0.437	3.802		3.805 (3.805)	3.798	3.803	3.815	3.800 (3.849)	3.796	3.823	3.811	3.839 (3.799)	3.837
2D	0.396	4.150		4.164 (4.108)	4.160	4.196	4.165	4.159 (4.209)	4.099	4.190		4.187 (4.158)	4.210
3D	0.372	4.455		4.478 (4.336)	4.478	4.455	4.522		4.327			4.486 (4.473)	

Table 3. Hyperfine and fine splittings(in MeV). (LP = Linear potential model, SP = Screened potential model, NR = Non-relativistic and RE = Relativistic)

Splitting	This work	Expt. [4]	Others									
			[79] LP(SP)	[107]	[108]	[73] NR(GI)	[76]	[75]	[109]	[111] RE (NR)	[110]	[61]
$m(1^3S_1)-m(1^1S_0)$	99	113.3 ± 0.7	114 (113)	116	115	108 (123)	100	118	117	102 (108)	117	119
$m(2^3S_1)-m(2^1S_0)$	43	46.7 ± 1.3	44 (42)	11	51	42 (53)	38	50	89	33 (42)	98	54
$m(3^3S_1)-m(3^1S_0)$	36		30 (26)	9	50	29 (36)	29	31	81	30 (29)	97	32
$m(4^3S_1)-m(4^1S_0)$	34		24 (17)	6	26	22 (25)	20	23		24 (22)		4.3
$m(5^3S_1)-m(5^1S_0)$	32		21 (13)	6	26				17	22 (19)		2.3
$m(6^3S_1)-m(6^1S_0)$	32			5	12				10	19 (17)		
$m(1^3P_2)-m(1^3P_1)$	33	45.5 ± 0.2	36 (32)	47	44	51 (40)	41	44	50	41 (44)	46	
$m(1^3P_1)-m(1^3P_0)$	66	95.9 ± 0.4	101 (106)	63	102	81 (65)	52	77	92	71 (80)	86	
$m(2^3P_2)-m(2^3P_1)$	31		30 (23)	46	45	47 (26)	38	36	54	40 (40)	43	
$m(2^3P_1)-m(2^3P_0)$	59		68 (66)	59	36	73 (37)	92	59	96	66 (73)	75	
$m(3^3P_2)-m(3^3P_1)$	33		26 (19)	44	35	46 (20)	53	30		45 (38)		
$m(3^3P_1)-m(3^3P_0)$	60		54 (46)	58	18	69 (25)	81	47		63 (69)		

3 Results and Discussion

In the framework of Cornell potential with a Gaussian wave function and relativistic correction of the Hamiltonian, comprise with a $\mathcal{O}(1/m)$ rectification in the potential energy term and elaboration of the kinetic energy term up to $\mathcal{O}(\mathbf{p}^{10})$, we have studied the mass spectra of charmonium states. We have calculated center of weight masses (value of Hamiltonian yields) for the nS ($n \leq 6$), nP and nD ($n \leq 3$) charmonium states and tabulated in Table(2). We observed that Hamiltonian yields for nS ($n \leq 3$) and nP and nD ($n \leq 3$) are in accordance with experimental as well as values predicted by other theoretical model, whereas for nS ($4 \leq n \leq 6$) are underestimated and/or overestimated compared to results of other theoretical model.

The calculated mass of charmonium states are graphically represented in Fig.1 and tabulated in Table(4) with experimentally observed results. After addition of the spin hyperfine interaction in fixed spin average mass for the ground state, we obtained pseudoscalar state mass η_c (2995 MeV) and vector state mass J/ψ (3094 MeV). The estimated mass 2^1S_0 (3606 MeV) is 33 MeV lower than experimentally observed mass, whereas mass 3^3S_1 (4036) is accordance with mass given in PDG [4] and other model estimates [75, 79, 113]. Our calculated mass 5^3S_1 (4654 MeV) is 11 MeV higher than value quoted in PDG [4] and accordance with mass estimated by other model [109, 111]. We have assigned $X(4660)$ to the 5^3S_1 state of charmonium. Estimated mass of 6^3S_0 (4893 MeV) and 6^3S_1 (4925 MeV) states are agreement with mass estimated by other model [111].

The P-wave states, 1^3P_1 with predicted mass 3511

MeV, 1^1P_1 with predicted mass 3525 MeV and 2^3P_2 with predicted mass 3556 MeV are in good agreement with experimental observed value [4].

We have assigned newly observed charmonium like state $X(3900)$ to the 2^1P_1 (3936 MeV) and state $X(3872)$ to the 2^3P_1 (3925 MeV). The mass predicted for state 2^1P_1 (3936 MeV) and state 2^3P_1 (3925 MeV) is in good agreement with mass predicted by other model [65, 73, 76, 79, 107, 111, 113]. The candidate $X(3872)$ as the 2^3P_1 state with well established quantum numbers, although the interpretation of it as a molecular state [124, 125] and was questioned in Ref.[126], while Ref.[127] interpreted it as virtual state.

We have also assigned charmonium like states, $X(3915)$ and $X(4274)$ to the 2^3P_0 (3866 MeV) and 3^3P_1 (4257 MeV) states respectively. To consider $X(3915)$ as the 2^3P_0 state is still problematic and was also pointed out in Ref.[79, 128] and the references therein. In Ref.[128–130], the authors suggest the $X(3915)$ as the 2^3P_0 state faces the following problems: First, A scalar meson should be the open-flavor modes for the dominant decay channels, above the corresponding thresholds. The Facts that $X(3915)$ can couple in an S-wave and the $D\bar{D}$ channel, although was not observed in the $D\bar{D}$ channel. Second, the mass splitting between the state 1^3P_2 and 1^3P_0 is 141 MeV, while the mass splitting between relatively well determined $X(3930)$ as the 2^3P_2 state and $X(3915)$ as the 2^3P_0 state is 9 MeV, which is too small for the hyperfine splitting.

We observed that new charmonium like states $X(4140)$ and $X(4274)$ with their quantum number

Table 4. Complete mass spectra (in GeV). (LP = Linear potential model, SP = Screened potential model, NR = Non-relativistic and RE = Relativistic,)

State $n^{2S+1}L_J$	J^P	This work	Expt. [4]	Others									
				LP (SP) [79]	[107]	[113]	NR (GI) [73]	[76]	[75]	[109]	[110]	RE (NR)[111]	[112]
1^1S_0	0^{-+}	2.995	2.984	2.983 (2.984)	3.069	2.981	2.982 (2.975)	2.978	2.979	2.980	2.979	2.992 (2.982)	2.97
1^3S_1	1^{--}	3.094	3.097	3.097 (3.097)	3.097	3.096	3.090 (3.098)	3.088	3.097	3.097	3.096	3.094 (3.090)	3.10
2^1S_0	0^{-+}	3.606	3.639	3.635 (3.637)	3.659	3.635	3.630 (3.623)	3.647	3.623	3.597	3.588	3.625 (3.630)	3.62
2^3S_1	1^{--}	3.649	3.686	3.679 (3.679)	3.670	3.686	3.672 (3.676)	3.685	3.673	3.686	3.686	3.668 (3.672)	3.68
3^1S_0	0^{-+}	4.000		4.048 (4.004)	4.063	3.989	4.043 (4.064)	4.058	3.991	4.014	3.991	4.029 (4.043)	4.06
3^3S_1	1^{--}	4.036	4.039	4.078 (4.030)	4.072	4.039	4.072 (4.100)	4.087	4.022	4.095	4.088	4.059 (4.072)	4.10
4^1S_0	0^{-+}	4.328		4.388 (4.264)	4.403	4.401	4.384 (4.425)	4.391	4.250			4.332 (4.388)	
4^3S_1	1^{--}	4.362	4.421	4.412 (4.281)	4.409	4.427	4.406 (4.450)	4.411	4.273	4.433		4.356 (4.406)	4.45
5^1S_0	0^{-+}	4.622		4.690 (4.459)	4.705	4.811			4.446			4.639 (4.685)	
5^3S_1	1^{--}	4.654	4.643	4.711 (4.472)	4.711	4.837			4.463			4.661 (4.704)	
6^1S_0	0^{-+}	4.893			4.983	5.155			4.595			4.893 (4.960)	
6^3S_1	1^{--}	4.925			4.988	5.167			4.605			4.912 (4.977)	
1^3P_0	0^{++}	3.457	3.415	3.415 (3.415)	3.440	3.413	3.424 (3.445)	3.366	3.433	3.416	3.424	3.472 (3.424)	3.44
1^3P_1	1^{++}	3.523	3.511	3.516 (3.521)	3.503	3.511	3.505 (3.510)	3.518	3.510	3.508	3.510	3.543 (3.505)	3.51
1^1P_1	1^{+-}	3.534	3.525	3.522 (3.526)	3.526	3.525	3.516 (3.517)	3.527	3.519	3.527	3.526	3.544 (3.516)	3.52
1^3P_2	2^{++}	3.556	3.556	3.552 (3.553)	3.550	3.555	3.556 (3.550)	3.559	3.554	3.558	3.556	3.584 (3.549)	3.55
2^3P_0	0^{++}	3.866	3.918	3.869 (3.848)	3.862	3.870	3.852 (3.916)	3.843	3.842	3.844	3.854	3.885 (3.852)	3.92
2^3P_1	1^{++}	3.925	3.872	3.937 (3.914)	3.921	3.906	3.925 (3.953)	3.935	3.901	3.940	3.929	3.951 (3.925)	3.95
2^1P_1	1^{+-}	3.936	3.887	3.940 (3.916)	3.944	3.926	3.934 (3.956)	3.942	3.908	3.961	3.945	3.951 (3.934)	3.96
2^3P_2	2^{++}	3.956	3.927	3.967 (3.937)	3.967	3.949	3.972 (3.979)	3.973	3.937	3.994	3.972	3.994 (3.965)	3.98
3^3P_0	0^{++}	4.197		4.230 (4.146)	4.212	4.301	4.202 (4.292)	4.208	4.131			4.219 (4.202)	
3^3P_1	1^{++}	4.257	4.273	4.284 (4.192)	4.270	4.319	4.271 (4.317)	4.299	4.178			4.283 (4.271)	
3^1P_1	1^{+-}	4.269		4.285 (4.193)	4.292	4.337	4.279 (4.318)	4.310	4.184			4.283 (4.279)	
3^3P_2	2^{++}	4.290		4.310 (4.311)	4.314	4.354	4.317 (4.337)	4.352	4.208			4.328 (4.309)	
1^3D_1	1^{--}	3.799	3.773	3.787 (3.792)	3.759	3.783	3.785 (3.819)	3.809	3.787	3.804	3.798	3.830 (3.785)	3.82
1^3D_2	2^{--}	3.805	3.822	3.807 (3.807)	3.787	3.795	3.800 (3.838)	3.820	3.798	3.824	3.813	3.841 (3.800)	3.84
1^1D_2	2^{-+}	3.802		3.806 (3.805)	3.799	3.807	3.799 (3.879)	3.815	3.796	3.824	3.811	3.837 (3.799)	3.84
1^3D_3	3^{--}	3.801		3.811 (3.808)	3.823	3.813	3.806 (3.849)	3.813	3.799	3.831	3.815	3.844 (3.805)	3.84
2^3D_1	1^{--}	4.145	4.191	4.144 (4.095)	4.119	4.150	4.142 (4.194)	4.154	4.089	4.164		4.174 (4.141)	4.19
2^3D_2	2^{--}	4.152		4.165 (4.109)	4.148	4.190	4.158 (4.208)	4.169	4.100	4.189		4.187 (4.158)	4.21
2^1D_2	2^{-+}	4.150		4.164 (4.108)	4.160	4.196	4.158 (4.208)	4.165	4.099	4.191		4.183 (4.158)	4.21
2^3D_3	3^{--}	4.151		4.172 (4.112)	4.185	4.220	4.167 (4.217)	4.166	4.103	4.202		4.195 (4.165)	4.22
3^3D_1	1^{--}	4.448		4.456 (4.324)	4.437	4.448		4.502	4.317	4.477		4.470 (4.455)	4.52
3^3D_2	2^{--}	4.456		4.478 (4.337)	4.466	4.456		4.524	4.327			4.485 (4.472)	
3^1D_2	2^{-+}	4.455		4.478 (4.336)	4.478	4.455		4.524	4.326			4.480 (4.472)	
3^3D_3	3^{--}	4.457		4.486 (4.340)	4.503	4.457		4.527	4.331			4.497 (4.481)	

Table 5. Electric dipole (E1) transitions widths of $c\bar{c}$ mesons. (LP = Linear potential model, SP = Screened potential model, NR = Non-relativistic and RE = Relativistic, Here E_γ in MeV and Γ in KeV)

Transition		This work		Expt.[4]	Other work									
Initial	Final	E_γ	Γ	Γ	[75]	[110]	[114]	[73]	[115]	[116]	[77]	[76]	[79]	[111]
					NR(GI)									
					LP(SP)									
					RE(NR)									
1^3P_2	1^3S_1	432.31	233.85	406 ± 31	309	327	383	424 (313)	315	315		405	327(338)	437.5(424.5)
1^3P_1	1^3S_1	402.92	189.86	320 ± 25	244	265	361	314 (239)	241	242		341	269 (278)	329.5(319.5)
1^1P_1	1^1S_0	497.67	357.83		323	560	671	498 (352)	482	482		473	361 (373)	570.5(490.3)
1^3P_0	1^3S_1	344.13	118.29	131 ± 14	117	121	264	152 (114)	120	120		104	141(146)	159.2(154.5)
2^3S_1	1^3P_2	91.58	7.07	26 ± 1.5	34	18.2		38 (24)	30.1	29	28.6	39	36(44)	35.5 (37.9)
2^3S_1	1^3P_1	123.46	10.39	27.9 ± 1.5	36	22.9		54 (29)	42.8	41	33.0	38	45(48)	50.9 (54.2)
2^3S_1	1^1P_1	112.88	7.94		104									
2^3S_1	1^3P_0	186.43	11.93	29.8 ± 1.5	25	26.3		63 (26)	47	46	28.8	29	27(26)	58.8 (62.6)
2^1S_0	1^3P_1	82.19	9.20											
2^1S_0	1^1P_1	71.49	6.05			6.2		49 (36)	35.1	35.1		56	49 (52)	45.2 (49.9)
1^3D_3	1^3P_2	237.31	237.51		323	156	432	272 (296)	402			302		397.7(271.1)
1^3D_2	1^3P_2	241.19	62.34		55	59	131	64 (66)	69.5	56		82	79(82)	96.52(64.06)
1^3D_2	1^3P_1	271.75	89.18		208	215	423	307 (268)	313	260		301	281(291)	438.2(311.2)
1^3D_1	1^3P_2	235.48	6.45	< 21	4.6	6.9	15.2	4.9 (3.3)	3.88	3.7	3.3	8.1	5.4 (5.7)	4.73(4.86)
1^3D_1	1^3P_1	266.10	139.52	70 ± 17	93	135	246	125 (77)	99	94	89.7	153	115 (111)	122.8(126.2)
1^3D_1	1^3P_0	326.57	343.87	172 ± 30	197	355	448	403 (213)	299	287	221.7	362	243 (232)	394.6(405.4)
2^3P_2	2^3S_1	295.70	281.93		100		164	304 (207)				264		377.1(287.5)
2^3P_1	2^3S_1	266.71	206.87		60		174	183 (183)				234		246.0(185.3)
2^1P_1	2^1S_0	315.84	343.55		108		333	280 (218)				274		349.8(272.9)
2^3P_0	2^3S_1	210.86	102.23		44		112	64 (135)				83		108.3(65.3)
2^3P_2	1^3D_3	152.16	33.27					88 (29)				76		60.67(78.69)
2^3P_2	1^3D_2	148.18	5.49					17 (5.6)				10		11.48(15.34)
2^3P_2	1^1D_2	151.21	5.83											
2^3P_2	1^3D_1	154.03	0.41					1.9 (1.0)				0.64		2.31(1.67)
2^3P_1	1^3D_1	123.91	5.35					22 (21)				11		31.15(21.53)
2^3P_0	1^3D_1	65.87	3.21					13 (51)				1.4		33.24(13.55)

Table 6. Magnetic dipole (M1) transitions widths. (LP = Linear potential model, SP = Screened potential model, NR = Non-relativistic and RE = Relativistic, Here E_γ in MeV and Γ in KeV)

Transition		This work		Expt.[4]	Other work								
Initial	Final	E_γ	Γ	Γ	[110]	[114]	NR(GI)[73]	[115]	[116]	[77]	[76]	LP(SP)[79]	RE(NR)[111]
1^3S_1	1^1S_0	97	1.647	1.58 ± 0.37	1.05	2.01	2.9 (2.4)	1.960	1.92	2.0	2.2	2.39 (2.44)	2.765 (2.752)
2^3S_1	2^1S_0	42	0.135	0.21 ± 0.15	0.99	0.20	0.21 (0.17)	0.140	0.04	0.2	0.096	0.19 (0.19)	0.198 (0.197)
3^3S_1	3^1S_0	36	0.082			0.012	0.046 (0.067)			0.0046	0.044	0.051 (0.088)	0.023 (0.044)
2^3S_1	1^1S_0	595	69.57	1.24 ± 0.29	0.95		4.6 (9.6)	0.926	0.91		3.8	8.08 (7.80)	3.370 (4.532)
2^1S_0	1^3S_1	476	35.72		1.12		7.9 (5.6)	0.538		7.2	6.9	2.64 (2.29)	5.792 (7.962)
1^3P_2	1^3P_0	97	1.638										
1^3P_2	1^3P_1	33	0.189										
1^3P_2	1^1P_1	22	0.056										
1^1P_1	1^3P_0	76	0.782										

Table 7. Leptonic decay widths ($\psi \rightarrow \Gamma_{e^+e^-}$ in KeV).

State	This work		Expt.[4]	Other work								
	$\Gamma_{l^+l^-}$	$\Gamma_{l^+l^-}^{cf}$		[117]	[105, 118]	[75]	[119]	[109]	[73]	[77]	[76]	[61]
J/ψ	8.335	3.623	$5.55 \pm 0.14 \pm 0.02$	3.112	6.847 (2.536)	11.8 (6.60)	4.080	4.28	12.13	3.93	6.0(3.3)	5.63
$\psi(2S)$	2.496	1.085	2.33 ± 0.07	2.197	3.666 (1.358)	4.29 (2.40)	2.375	2.25	5.03	1.78	2.2(1.2)	2.19
$\psi(3S)$	1.722	0.748	0.86 ± 0.07	1.701	2.597 (0.962)	2.53 (1.42)	0.835	1.66	3.48	1.11	1.8(0.98)	1.20
$\psi(4S)$	1.378	0.599	0.58 ± 0.07		2.101 (0.778)	1.73 (0.97)		1.33	2.63	0.78	1.3(0.70)	0.63
$\psi(5S)$	1.168	0.508			1.701 (0.633)	1.25 (0.70)					0.57	0.24
$\psi(6S)$	1.017	0.442				0.88 (0.49)					0.42	
1^3D_1	0.261	0.113	0.262 ± 0.018	0.275	0.096	0.055 (0.031)		0.09	0.056	0.22	0.079(0.044)	
2^3D_1	0.381	0.166	0.48 ± 0.22	0.223	0.112	0.066 (0.037)		0.16	0.096	0.30	0.13(0.073)	
3^3D_1	0.485	0.211				0.079 (0.044)				0.33		

Table 8. Two-photon decay widths without and with correction factor (in KeV).

State	This work		Expt.[4]	Other work											
	$\Gamma_{\gamma\gamma}$	$\Gamma_{\gamma\gamma}^{cf}$		[117]	[106]	[105, 118]	[75]	[120]	[121]	[92]	[122]	[119]	[76]	[123]	[121]
$\eta_c(1S)$	10.351	6.621	5.1 ± 0.4	6.96	7.918	6.68	8.5	5.09	3.5	7.18	7.14	4.252	7.5	5.5	3.5
$\eta_c(2S)$	4.501	2.879	2.15 ± 0.6	10.45	5.789	5.08	2.4	2.63	1.38	1.71	4.44	3.306	2.9	1.8	1.38
$\eta_c(3S)$	3.821	2.444		1.03	0.299	4.53	0.88		0.94	1.21		1.992	2.5		
$\eta_c(4S)$	3.582	2.291							0.73				1.8		
$\eta_c(5S)$	3.460	2.213							0.62						
$\eta_c(6S)$	3.378	2.161													
1^3P_0	1.973	2.015	2.36 ± 0.35	13.43		2.62	2.5	2.02	1.39	3.28			10.8	2.9	1.39
2^3P_0	2.299	2.349		2.67			1.7		1.11				6.7	1.9	1.11
3^3P_0	2.714	2.773					1.2		0.91				6.5		
1^3P_2	0.526	0.229	0.53 ± 0.03	1.72		0.25	0.31	0.46	0.44				0.27	0.50	0.44
2^3P_2	0.613	0.267		0.343			0.23		0.48				0.39	0.52	0.48
3^3P_2	0.724	0.315					0.17		0.014				0.66		

Table 9. Three-photon decay widths (in eV).

State	This work		Expt.[4]
	$\Gamma_{\gamma\gamma\gamma}$	$\Gamma_{\gamma\gamma\gamma}^{cf}$	
J/ψ	4.41691	3.94748	1.08 ± 0.032
$\psi(2S)$	1.83911	1.64365	
$\psi(3S)$	1.55252	1.38752	
$\psi(4S)$	1.45187	1.29756	
$\psi(5S)$	1.40027	1.25145	
$\psi(6S)$	1.36564	1.2205	

Table 10. Three-gluon decay widths (KeV) .

State	This work		Expt.[4]	Other work	
	Γ_{ggg}	Γ_{ggg}^{cf}		[116]	[31]MeV
J/ψ	442.669	269.059	59.55 ± 0.18	52.8 ± 5	
$\psi(2S)$	184.318	112.031	31.38 ± 0.85	23 ± 2.6	
$\psi(3S)$	155.596	94.5727			
$\psi(4S)$	145.508	88.4413			
$\psi(5S)$	140.337	85.2984			
$\psi(6S)$	136.866	83.1888			
1^1P_1	285.127			720 ± 320	
2^1P_1	420.078				1.29
3^1P_1	558.78				
1^3D_1	189.367			216	1.15
2^3D_1	359.346				
3^3D_1	556.588				
1^3D_2	53.8761			36	0.08
2^3D_2	102.236				
3^3D_2	158.353				
1^3D_3	89.7001			102	0.18
2^3D_3	170.217				
3^3D_3	263.647				

Table 11. Two-gluon decay widths(in MeV).

State	This work		Expt.[4]	Other work					
	Γ_{gg}	Γ_{gg}^{cf}		[117]	[106]	[105, 118]	[120]	[122]	[116]
$\eta_c(1S)$	24.249	36.587	28.6 ± 2.2	28.60	13.070	32.44	15.70	19.6	17.4 ± 2.8
$\eta_c(2S)$	10.545	15.910	14 ± 7	42.90	9.534	24.64	8.10	12.1	8.3 ± 1.3
$\eta_c(3S)$	8.952	13.507		4.26	4.412	21.99			
$\eta_c(4S)$	8.392	12.662							
$\eta_c(5S)$	8.106	12.230							
$\eta_c(6S)$	7.914	11.941							
1^3P_0	4.621	9.274	10 ± 0.6	47.76		15.67	4.68		14.3 ± 3.6
2^3P_0	5.386	10.810		9.50					
3^3P_0	6.357	12.758							
1^3P_2	1.232	0.945	1.97 ± 0.11	5.27		1.46	1.72		1.71 ± 0.21
2^3P_2	1.436	1.101		1.04					
3^3P_2	1.695	1.300							
1^1D_2	12.460 (KeV)								110 (KeV)
2^1D_2	21.679 (KeV)								
3^1D_2	31.757 (KeV)								

Table 12. $n^3S_1 \rightarrow \gamma gg$ decay widths.

State	This work		Expt.[4]
State	$\Gamma_{\rightarrow\gamma gg}$ (KeV)	$\Gamma_{\rightarrow\gamma gg}^{cf}$ (KeV)	
J/ψ	31.0421	8.99657	8.18 ± 0.25
$\psi(2S)$	12.9253	3.74599	2.93 ± 0.16
$\psi(3S)$	10.9111	3.16224	
$\psi(4S)$	10.2037	2.95723	
$\psi(5S)$	9.8411	2.85214	
$\psi(6S)$	9.59771	2.7816	

 Table 13. $n^3P_1 \rightarrow q\bar{q} + g$ decay widths.

State	This work
	$\Gamma_{q\bar{q}+g}$ (KeV)
1^3P_1	342.152
2^3P_1	504.093
3^3P_1	670.536

$J^{PC} = 1^{++}$ is a good candidate for 3^3P_1 state within screen potential model and linear potential model respectively. However none of the **models** can give $J^{PC} = 1^{++}$ charmonium state masses 4147 MeV and 4273 MeV at the same time, which may indicate the exotic nature of $X(4140)$ and/or $X(4274)$, which was also pointed out in Ref.[79].

The predicted mass for 1^3D_1 (3799 MeV), 1^3D_2 (3805 MeV) and 2^3D_1 (4145 MeV) states are accordance with Experiment observed results [4] as well as with good agreement with other model prediction. [65, 73, 75, 76, 79, 111, 113]. The estimated masses of charmonium using our model are overall in agreement (with few MeV difference) with experimentally observed values. It is found that states with a mass of $M < 4.1$ GeV are in good agreement with other theoretical estimates.

Table(3) shows the hyperfine splittings for S wave states and fine splittings for some P wave states. For comparison, the experimental data from the PDG [4] and predictions with other theoretical model are listed in the same table as well. we observed that the predicted hyperfine splittings, up-to 2S states are in agreement with the world average data [4] and predictions with other theoretical model. The hyperfine splittings for 3S to 6S states have a different value in the different theoretical model. By comparing our predicted results with other theoretical model, we observed that masses of the low-lying nS ($n \leq 2$), nP , nD ($n = 1$), charmonium states are in less difference, whereas masses of the higher charmonium states nS ($n \geq 3$), nP , nD ($n \geq 2$), are in notable difference.

The estimated pseudoscalar and vector decay con-

stant $f_P(f_{Pcor})$ and $f_V(f_{Vcor})$ respectively, without(with) QCD correction are tabulated in Table(1), which are in agreement with experimental results as well as other theoretical model estimates.

We calculate radiative E1 and M1 dipole transitions widths and are tabulated in Tables(5, 6). We calculate the E1 transition of $\Gamma[1P \rightarrow (1S)\gamma]$, $\Gamma[2S \rightarrow (1P)\gamma]$, $\Gamma[1D \rightarrow (1P)\gamma]$, $\Gamma[2P \rightarrow (2S)\gamma]$ and $\Gamma[2P \rightarrow (1D)\gamma]$ using the masses predicted by our model. Our calculated E1 transition of $\Gamma[1P \rightarrow (1S)\gamma]$ and $\Gamma[2S \rightarrow (1P)\gamma]$ are lesser than experimental results as well as other theoretical estimates, whereas for $\Gamma[1D \rightarrow (1P)\gamma]$, $\Gamma[2P \rightarrow (2S)\gamma]$ and $\Gamma[2P \rightarrow (1D)\gamma]$ transition, are in agreement with the estimates of other theoretical model. Our prediction of $\Gamma[1^3D_1 \rightarrow (1^3P_1)\gamma]$ and $\Gamma[1^3D_1 \rightarrow (1^3P_0)\gamma]$ almost double in comparison with the PDG average data [4] while prediction of $\Gamma[1^3D_1 \rightarrow (1^3P_2)\gamma]$ is in agreement with the PDG average data [4] as well as with predicted by other model.

We also, calculate the M1 transition of the low-lying 1S, 2S and 3S states as well as 1P states. Our prediction of $\Gamma[1^3S_1 \rightarrow (1^1S_0)\gamma]$ and $\Gamma[2^3S_1 \rightarrow (2^1S_0)\gamma]$ are in agreement with the PDG average data [4], while $\Gamma[2^3S_1 \rightarrow (1^1S_0)\gamma]$ is much larger than the PDG average data [4]. **Gang Li and Qiang Zhao, Ref.[131, 132] studied intermediate meson loop contributions to $1^3S_1, 2^3S_1 \rightarrow \gamma 2^1S_0, (\gamma 1^1S_0)$ apart from the dominant M1 transitions in an effective Lagrangian approach. Results shows that the IML contributions are relatively small but play a crucial role. Radiative decay widths including the M1 in the GI model and intermediate hadronic loops for $1^3S_1 \rightarrow \gamma 2^1S_0$ is 1.59 KeV and for $2^3S_1 \rightarrow$**

$\gamma 2^1S_0(\gamma 1^1S_0)$ is **0.032(0.86) KeV [131]**, whereas **results including the M1 transition amplitude of the GI model and IML transitions for $1^3S_1 \rightarrow \gamma 2^1S_0$ is 1.58 ± 0.37 KeV and for $2^3S_1 \rightarrow \gamma 2^1S_0(\gamma 1^1S_0)$ is 0.08 ± 0.03 ($2.78^{+2.65}_{-1.75}$) KeV [132]**.

Our prediction of $\Gamma[3^3S_1 \rightarrow (3^1S_0)\gamma]$ is in agreement with the other theoretical model prediction, while prediction of $\Gamma[2^1S_0 \rightarrow (1^3S_1)\gamma]$ is larger than the predicted by other theoretical model. We observed that the various models have different estimates of E1 and M1 transitions, it may be due to the different models have different parameters or treatments in the relativistic corrections. The E1 and M1 transitions as a whole are strongly model dependence and more studies are required in both experiments as well theory.

We estimate partial decay width Γ and Γ^{cf} (with QCD correction factor) of annihilation processes, using the masses predicted by our potential model and the radial wave function at the origin, for e^+e^- , two-photon, three-photon, two-gluon, three-gluon, γgg and $q\bar{q}+g$ are tabulated in Tables(7-13) and are compared with experimental results from PDG[4] as well as other theoretically calculated estimates.

We observed that our estimated leptonic decay without QCD correction for J/ψ , $\psi(2S)$, $\psi(3S)$ and $\psi(4S)$ is higher than experimentally observed leptonic decay width. **After QCD correction, estimated leptonic decay is 1.93 KeV, 1.24 KeV, 0.11 KeV and 0.019 KeV** lesser than the experimental result for J/ψ , $\psi(2S)$, $\psi(3S)$ and $\psi(4S)$ state respectively. Also, our estimated leptonic decay with QCD correction for n^3D_1 state is much lower than the experimental result.

Our estimated two-photon and two-gluon decay widths with QCD correction for $\eta_c(nS)$, n^3P_0 and n^3P_2 state are accordance with experimentally observed results as well as with the other theoretical estimates. Our estimated three-photon decay widths with QCD correction for J/ψ is lower than the experimentally observed result whereas estimated three-gluon decay widths with QCD correction for J/ψ and $\psi(2S)$ state is higher than the experimentally observed result as well as other theoretical estimates.

Our estimated γgg decay width with QCD correction for J/ψ and $\psi(2S)$ state is **accordance** with the experimentally observed result. We have also **compute** $q\bar{q}+g$ decay width for n^3P_1 states. We observed that radiative QCD corrections modify theoretical predictions considerably and **bring** estimated result close to experimental data. We also observed that the estimated values of annihilation decay width by of various models show a

wide range of variations. Due to the considerable uncertainties arise from the wave functions dependence model and possible relativistic as well as QCD radiative corrections, we would like to mention that formulas used for calculation of annihilation decay width should be regarded as estimates of the partial widths rather than precise predictions.

3.1 Regge trajectories

We plot the Regge trajectories for the (n, M^2) and (J, M^2) planes with the help of masses estimated by our potential model. The "daughter" trajectories are the trajectories with the same value of J and differ by a quantum number correspondent to the radial quantum number. The masses of the "daughter" trajectories are higher than those for the leading trajectory with given quantum numbers. The linearity of Regge trajectories **represents** as a reflection of strong forces between quarks at large distances (color confinement).

The Regge trajectories in the (J, M^2) plane with $(P = (-1)^J)$ ($J^P = 1^-, 2^+, 3^-$) natural and $(P = (-1)^{J-1})$ ($J^P = 0^-, 1^+, 2^-$) unnatural parity are depicted in Figs. (2-3). **In figure, charmonium masses estimated by our model are represented by the solid triangles whereas experimentally available mass with the corresponding charmonium name are represented by hollow squares.** The Regge trajectories for $n_r = n - 1$ principal quantum number in the (n_r, M^2) plane are describe in Figure (4) and Figure (5).

The following definitions are used to calculate the χ^2 fitted slopes (α , β) and the intercepts (α_0 , β_0) [82, 83].

$$J = \alpha M^2 + \alpha_0. \quad (39)$$

$$n_r = \beta M^2 + \beta_0 \quad (40)$$

Calculated slopes and intercepts are tabulated in Tables (14,15,16). The estimated masses of the charmonium fit well to the (n, M^2) and (J, M^2) planes trajectories. The daughter trajectories, which involve both radially and orbitally excited states, turn out to be almost linear, equidistant and parallel whereas The parent Regge trajectories, which start from ground states, are exhibiting a nonlinear behavior in the lower mass region in both planes.

We observed that the linearity of the Regge trajectories depends on quark masses, as the orbital momentum ℓ of the state is proportional to its mass: $\ell = \alpha M^2(\ell) + \alpha(0)$, where the slope α depends on the flavor content of the states lying on the corresponding trajectory. In the Regge phenomenology, the radial spectrum of heavy quarkonia typically **leads** to strong nonlinearities, in the framework of hadron string model [133].

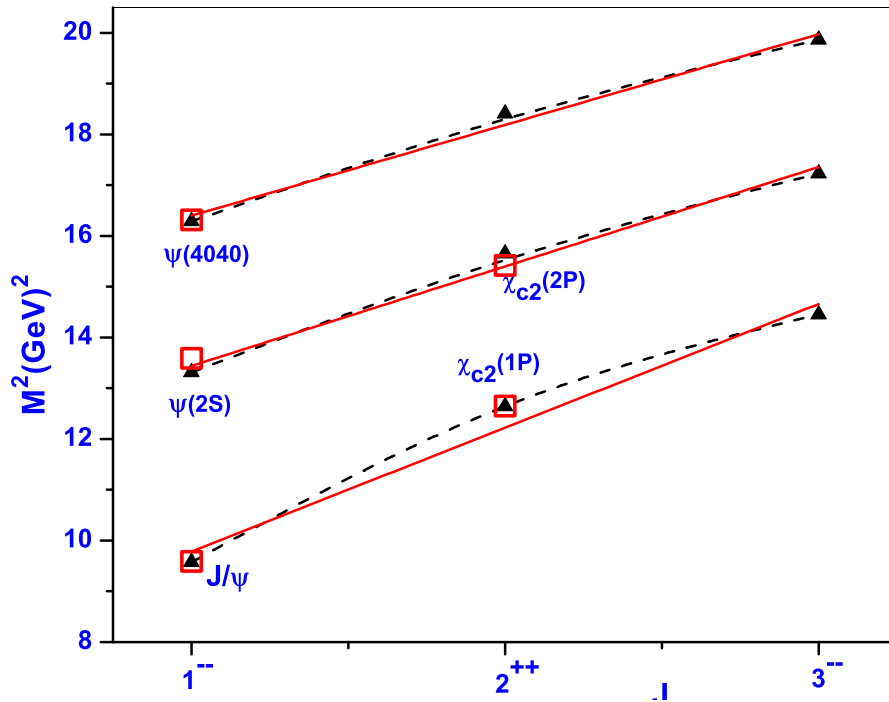


Fig. 2. Regge trajectory ($M^2 \rightarrow J$) with natural parity.

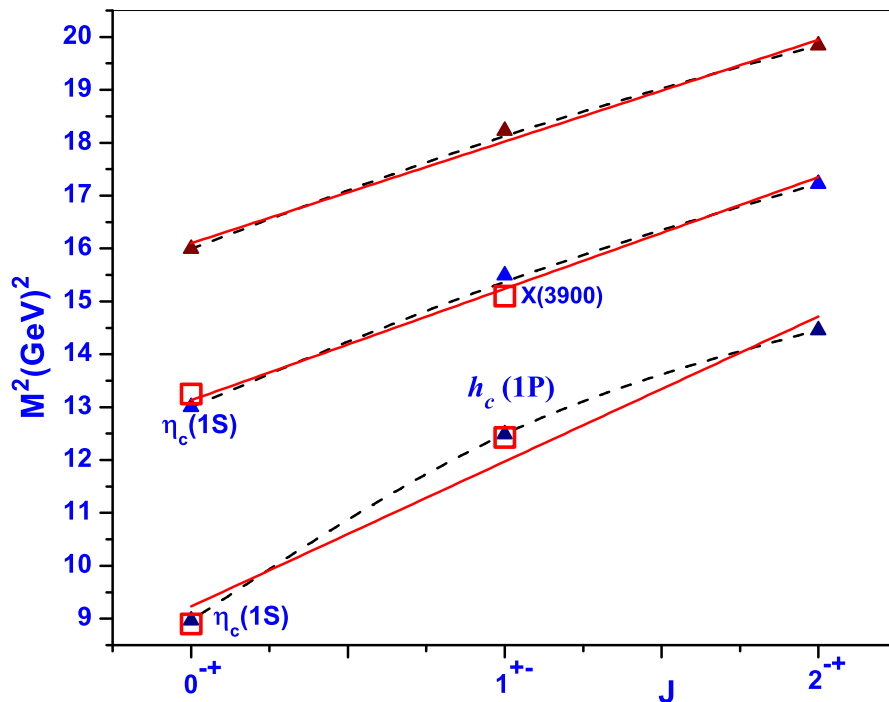


Fig. 3. Regge trajectory ($M^2 \rightarrow J$) with unnatural parity.

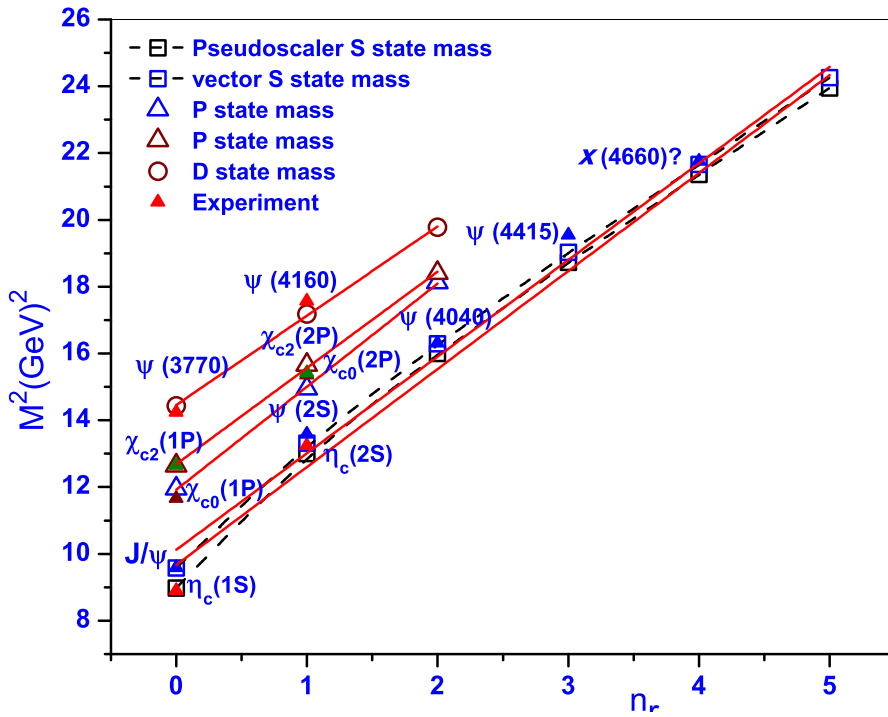


Fig. 4. Regge trajectory ($M^2 \rightarrow n_r$) for the pseudoscalar and vector S state and excited P and D state masses.

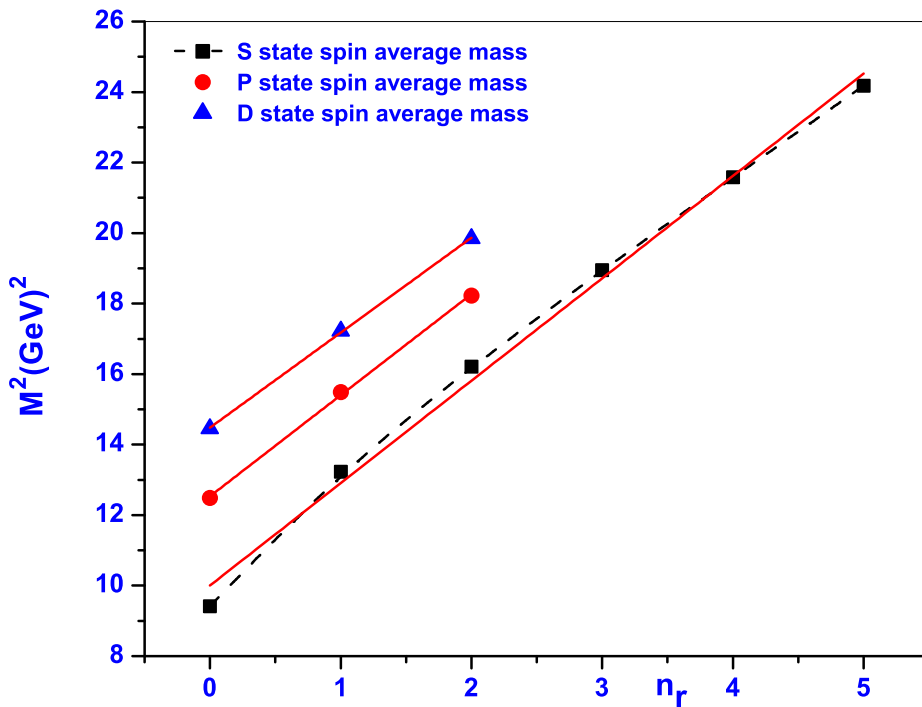


Fig. 5. Regge trajectory ($M^2 \rightarrow n_r$) for the S-P-D states center of weight mass.

Table 14. Slopes and intercepts of the (J, M^2) Regge trajectories with unnatural and natural parity.

Parity	Trajectory	$\alpha(GeV^{-2})$	α_0
Unnatural	Parent	0.355 ± 0.058	-3.252 ± 0.706
	First daughter	0.471 ± 0.038	-6.164 ± 0.576
	Second daughter	0.518 ± 0.032	-8.319 ± 0.570
Natural	Parent	0.401 ± 0.060	-2.902 ± 0.746
	First daughter	0.504 ± 0.057	-5.764 ± 0.877
	Second daughter	0.553 ± 0.059	-8.057 ± 1.081

Table 15. Slopes and intercepts for the (n_r, M^2) Regge trajectories.

Meson	J^P	$\beta(GeV^{-2})$	β_0
η_c	0^{-+}	0.341 ± 0.017	-3.236 ± 0.303
Υ	1^{--}	0.347 ± 0.014	-3.463 ± 0.252
χ_{c0}	0^{++}	0.324 ± 0.006	-3.861 ± 0.088
χ_{c1}	1^{++}	0.355 ± 0.007	-4.441 ± 0.112
h_c	1^{+-}	0.346 ± 0.009	-4.399 ± 0.138
χ_{c2}	2^{++}	0.345 ± 0.012	-4.284 ± 0.183
$\psi(^3D_1)$	1^{--}	0.374 ± 0.006	-5.406 ± 0.104
$\psi(^3D_2)$	2^{--}	0.377 ± 0.009	-5.473 ± 0.159
$\psi(^1D_2)$	2^{-+}	0.371 ± 0.006	-5.372 ± 0.101
$\psi(^3D_3)$	3^{--}	0.369 ± 0.006	-5.344 ± 0.100

Table 16. Slopes and intercepts of (n_r, M^2) Regge trajectory for center of weight mass.

Trajectory	$\beta(GeV^{-2})$	β_0
S State	0.342 ± 0.012	-3.413 ± 0.226
P State	0.348 ± 0.009	-4.36 ± 0.1464
D State	0.371 ± 0.006	-5.372 ± 0.101

4 Conclusion

We can conclude from the mass spectra of charmonium, Tables (2,4), investigated using a Cornell potential with relativistic correction to the Hamiltonian, are accordance with the available experimental results as well as predicted by the other theoretical model. The predicted pseudoscalar ($f_{P_{cor}}$) and the vector ($f_{V_{cor}}$) decay constants with QCD correction using our estimated charmonium masses are in accordance with experimental as well as predicted by other theoretical model.

We observed from the Regge trajectories Figs. (2-5), that the experimental masses of charmonium states are sitting nicely. In the mass region of the lowest excitations of charmonium, the slope of the trajectories decreases with increasing quark mass. The curvature of the trajectory near the ground state is due to the contribution of the color Coulomb interaction, which increases with mass. Hence, the Regge trajectories of the charmonium are basically nonlinear and exhibiting a nonlinear behavior in the lower mass region.

From a comparison of our estimated radiative (E1 and M1 dipole) transitions width with other theoretical estimations, we conclude that the various models have very different predictions of E1 and M1 dipole transitions may be due to different parameters and treatments are used in the relativistic corrections in the model. The calculated E1 and M1 dipole transitions width using the masses and parameters estimated by our model are in agreement with other theoretical and experimental predictions. Although, in most cases, more precise experimental measurements are required.

We also conclude from calculated annihilation decay widths using the Van Royen-Weisskopf relation, that the inclusion of QCD correction factors is helpful to bring estimated results close to experimental results. The various models show a wide range of variations in results of annihilation decay widths, which may be resolved using the NRQCD (non-relativistic QCD) and pNRQCD (potential non-relativistic QCD) formalism.

Acknowledgements A. K. Rai acknowledge the financial support extended by Department of Science of Technology, India under SERB fast track scheme SR/FTP /PS-152/2012.

References

- 1 J.J. Aubert et al. (E598), Phys. Rev. Lett. **33**, 1404 (1974)
- 2 J.E. Augustin et al. (SLAC-SP-017), Phys. Rev. Lett. **33**, 1406 (1974)
- 3 N. Brambilla, S. Eidelman, B. Heltsley, R. Vogt, G. Bodwin et al., Eur. Phys. J. **C71**, 1534 (2011)
- 4 C. Patrignani, P.D. Group, Chinese Physics C **40**, 100001 (2016)
- 5 J. Siegrist et al., Phys. Rev. Lett. **36**, 700 (1976)
- 6 R. Brandelik et al. (DASP), Phys. Lett. **76B**, 361 (1978)
- 7 E. Eichten, K. Gottfried, T. Kinoshita, K.D. Lane, T.M. Yan, Phys. Rev. D **21**, 203 (1980)
- 8 R. Aaij et al. (LHCb), Phys. Rev. Lett. **111**, 101805 (2013)
- 9 X.L. Wang et al. (Belle), Phys. Rev. Lett. **99**, 142002 (2007)
- 10 G. Pakhlova et al. (Belle), Phys. Rev. Lett. **101**, 172001 (2008)
- 11 P.A. Rapidis et al., Phys. Rev. Lett. **39**, 526 (1977)
- 12 W. Bacino et al., Phys. Rev. Lett. **40**, 671 (1978)
- 13 G.S. Abrams et al., Phys. Rev. **D21**, 2716 (1980)
- 14 M. Ablikim et al. (BES), Phys. Lett. **B652**, 238 (2007)
- 15 V.V. Anashin et al., Phys. Lett. **B711**, 292 (2012)
- 16 K. Abe et al. (Belle), Phys. Rev. Lett. **98**, 082001 (2007)
- 17 P. Pakhlov et al. (Belle), Phys. Rev. Lett. **100**, 202001 (2008)
- 18 W. Sreethawong, K. Xu, Y. Yan (2013), **1306.2780**
- 19 Z.H. Wang, Y. Zhang, L. Jiang, T.H. Wang, Y. Jiang, G.L. Wang, Eur. Phys. J. **C77**(1), 43 (2017)
- 20 V. Bhardwaj et al. (Belle), Phys. Rev. Lett. **111**(3), 032001 (2013)
- 21 M. Ablikim et al. (BESIII), Phys. Rev. Lett. **115**(1), 011803 (2015)
- 22 S.K. Choi et al. (Belle), Phys. Rev. Lett. **91**, 262001 (2003)
- 23 D. Acosta et al. (CDF), Phys. Rev. Lett. **93**, 072001 (2004)
- 24 V.M. Abazov et al. (D0), Phys. Rev. Lett. **93**, 162002 (2004)
- 25 B. Aubert et al. (BaBar), Phys. Rev. **D71**, 071103 (2005)
- 26 S.K. Choi et al., Phys. Rev. **D84**, 052004 (2011)
- 27 T. Aaltonen et al. (CDF), Phys. Rev. Lett. **103**, 152001 (2009)
- 28 B. Aubert et al. (BaBar), Phys. Rev. **D77**, 111101 (2008)
- 29 A. Abulencia et al. (CDF), Phys. Rev. Lett. **98**, 132002 (2007)
- 30 M. Ablikim et al. (BESIII), Phys. Rev. Lett. **112**(9), 092001 (2014)
- 31 T. Barnes, S. Godfrey, Phys. Rev. **D69**, 054008 (2004)
- 32 S.K. Choi et al. (Belle Collaboration), Phys. Rev. Lett. **94**, 182002 (2005)
- 33 P. del Amo Sanchez et al. (BaBar), Phys. Rev. **D82**, 011101 (2010)
- 34 J.P. Lees et al. (BaBar), Phys. Rev. **D86**, 072002 (2012), **1207.2651**
- 35 X. Liu, Z.G. Luo, Z.F. Sun, Phys. Rev. Lett. **104**, 122001 (2010)
- 36 Z.Y. Zhou, Z. Xiao, H.Q. Zhou, Phys. Rev. Lett. **115**(2), 022001 (2015)
- 37 S. Uehara et al. (Belle), Phys. Rev. Lett. **96**, 082003 (2006)
- 38 B. Aubert et al. (BaBar), Phys. Rev. **D81**, 092003 (2010)
- 39 M. Ablikim et al. (BESIII), Phys. Rev. Lett. **110**, 252001 (2013)
- 40 Z.Q. Liu et al. (Belle), Phys. Rev. Lett. **110**, 252002 (2013)
- 41 T. Xiao, S. Dobbs, A. Tomaradze, K.K. Seth, Phys. Lett. **B727**, 366 (2013)
- 42 M. Ablikim et al. (BESIII), Phys. Rev. **D92**(9), 092006 (2015)
- 43 T. Aaltonen et al. (CDF), Phys. Rev. Lett. **102**, 242002 (2009)
- 44 S. Chatrchyan et al. (CMS), Phys. Lett. **B734**, 261 (2014)
- 45 V.M. Abazov et al. (D0), Phys. Rev. Lett. **115**(23), 232001 (2015)
- 46 V.M. Abazov et al. (D0), Phys. Rev. **D89**(1), 012004 (2014)
- 47 X. Liu, S.L. Zhu, Phys. Rev. **D80**, 017502 (2009), [Erratum: Phys. Rev. **D85**, 019902(2012)]
- 48 T. Branz, T. Gutsche, V.E. Lyubovitskij, Phys. Rev. **D80**, 054019 (2009)
- 49 R.M. Albuquerque, M.E. Bracco, M. Nielsen, Phys. Lett. **B678**, 186 (2009)
- 50 G.J. Ding, Eur. Phys. J. **C64**, 297 (2009)
- 51 F. Stancu, J. Phys. **G37**, 075017 (2010)
- 52 Z.g. Wang, Y.f. Tian, Int. J. Mod. Phys. **A30**, 1550004 (2015)
- 53 V.V. Anisovich, M.A. Matveev, A.V. Sarantsev, A.N. Semenova, Int. J. Mod. Phys. **A30**(32), 1550186 (2015)
- 54 Z.G. Wang, Eur. Phys. J. **C63**, 115 (2009)
- 55 N. Mahajan, Phys. Lett. **B679**, 228 (2009)
- 56 R. Aaij et al. (LHCb), Phys. Rev. **D85**, 091103 (2012)
- 57 J.P. Lees et al. (BaBar), Phys. Rev. **D89**(11), 112004 (2014)
- 58 T. Aaltonen et al. (CDF), Mod. Phys. Lett. **A32**(26), 1750139

- (2017)
- 59 R. Aaij et al. (LHCb), Phys. Rev. **D95**(1), 012002 (2017)
- 60 Q.F. L, Y.B. Dong, Phys. Rev. **D94**(7), 074007 (2016)
- 61 T. Bhavsar, M. Shah, P.C. Vinodkumar, Eur. Phys. J. **C78**(3), 227 (2018)
- 62 P. Gonzalez, Phys. Rev. **D92**, 014017 (2015)
- 63 P. Guo, T. Ypez-Martinez, A.P. Szczepaniak, Phys. Rev. **D89**(11), 116005 (2014)
- 64 H.W. Ke, X.Q. Li, Y.L. Shi, Phys. Rev. **D87**(5), 054022 (2013)
- 65 D. Ebert, R. Faustov, V. Galkin, Mod.Phys.Lett. **A17**, 803 (2002)
- 66 N. Brambilla, eConf **C0610161**, 004 (2006), hep-ph/0702105
- 67 F. De Fazio, Phys. Rev. **D79**, 054015 (2009), [Erratum: Phys. Rev. **D83**, 099901(2011)]
- 68 G.C. Donald, C. Davies et al., Phys. Rev. **D86**, 094501 (2012), 1208.2855
- 69 L. Liu, G. Moir, Peardon et al. (Hadron Spectrum), JHEP **07**, 126 (2012)
- 70 S.L. Zhu, Y.B. Dai, Phys. Rev. **D59**, 114015 (1999)
- 71 V.A. Beilin, A.V. Radyushkin, Nucl. Phys. **B260**, 61 (1985)
- 72 S. Godfrey, N. Isgur, Phys. Rev. D **32**, 189 (1985)
- 73 T. Barnes, S. Godfrey, E.S. Swanson, Phys. Rev. **D72**, 054026 (2005)
- 74 B.Q. Li, C. Meng, K.T. Chao (2012), 1201.4155
- 75 B.Q. Li, K.T. Chao, Phys. Rev. **D79**, 094004 (2009)
- 76 L. Cao, Y.C. Yang, H. Chen, Few Body Syst. **53**, 327 (2012)
- 77 J. Segovia, A.M. Yasser, D.R. Entem, F. Fernandez, Phys. Rev. **D78**, 114033 (2008)
- 78 E. Eichten et al., Phys. Rev. D **17**(11), 3090 (1978)
- 79 W.J. Deng, H. Liu, L.C. Gui, X.H. Zhong, Phys. Rev. **D95**(3), 034026 (2017)
- 80 S. Godfrey, K. Moats, Phys. Rev. **D92**(5), 054034 (2015)
- 81 Y. Koma, M. Koma, H. Wittig, Phys. Rev. Lett **97**, 122003 (2006)
- 82 V. Kher, N. Devlani, A.K. Rai (2017), 1704.00439
- 83 V. Kher, N. Devlani, A.K. Rai, Chinese Physics C **Vol. 41**,(No. 9), 093101 (2017)
- 84 N. Brambilla, A. Pineda, J. Soto, A. Vairo, Rev. Mod. Phys. **77**, 1423 (2005)
- 85 N. Brambilla et al., Eur. Phys. J. **C74**(10), 2981 (2014)
- 86 S.N. Gupta, J.M. Johnson, Phys. Rev. D **51**(1), 168 (1995)
- 87 D.S. Hwang, C. Kim, W. Namgung, Phys.Lett. **B406**, 117 (1997), hep-ph/9608392
- 88 A.K. Rai, B. Patel, P.C. Vinodkumar, Phys. Rev. C **78**(5), 055202 (2008)
- 89 A.K. Rai, R.H. Parmar, P.C. Vinodkumar, J. Phys. G: Nucl. Part. Phys. **28**(8), 2275 (2002)
- 90 E. Eichten, S. Godfrey, H. Mahlke, J.L. Rosner, Rev. Mod. Phys. **80**, 1161 (2008)
- 91 M.B. Voloshin, Prog. Part. Nucl. Phys. **61**, 455 (2008)
- 92 O. Lakhina, E.S. Swanson, Phys. Rev. D **74**, 014012 (2006)
- 93 R. Van Royen, V. Weisskopf, Nuovo Cim. **A50**, 617 (1967)
- 94 E. Braaten, S. Fleming, Phys. Rev. D **52**(1), 181 (1995)
- 95 D.S. Hwang, G.H. Kim, Phys. Rev. D **55**(11), 6944 (1997)
- 96 G.J. Ding, J.J. Zhu, M.L. Yan, Phys. Rev. **D77**, 014033 (2008)
- 97 Q.F. Lu, T.T. Pan, Y.Y. Wang, E. Wang, D.M. Li, Phys. Rev. **D94**(7), 074012 (2016)
- 98 F.K. Guo, C. Hanhart, G. Li, U.G. Meissner, Q. Zhao, Phys. Rev. **D82**, 034025 (2010)
- 99 S.F. Radford, W.W. Repko, M.J. Saelim, Phys. Rev. D **80**(3), 034012 (2009)
- 100 J. Segovia, P.G. Ortega, D.R. Entem, F. Fernandez, Phys. Rev. **D93**(7), 074027 (2016)
- 101 W. Kwong, P.B. Mackenzie, R. Rosenfeld, J.L. Rosner, Phys. Rev. **D37**, 3210 (1988)
- 102 W. Kwong, J.L. Rosner, Phys. Rev. **D38**, 279 (1988)
- 103 A. Bradley, A. Khare, Z. Phys. **C8**, 131 (1981)
- 104 G. Belanger, P. Moxhay, Phys. Lett. **B199**, 575 (1987)
- 105 Bhaghyesh, K.B. Vijaya Kumar, A.P. Monteiro, J. Phys. **G38**, 085001 (2011)
- 106 H. Negash, S. Bhatnagar, Int. J. Mod. Phys. **E25**(08), 1650059 (2016)
- 107 J.H. Yang, S.K. Lee, E.J. Kim, J.B. Choi (2015), 1506.04481
- 108 D. Ebert, R. Faustov, V. Galkin, Eur.Phys.J. **C71**, 1825 (2011)
- 109 S.F. Radford, W.W. Repko, Phys. Rev. **D75**, 074031 (2007)
- 110 D. Ebert, R.N. Faustov, V.O. Galkin, Phys. Rev. **D67**, 014027 (2003)
- 111 M.A. Sultan, N. Akbar, B. Masud, F. Akram, Phys. Rev. **D90**(5), 054001 (2014)
- 112 S. Godfrey, N. Isgur, Phys. Rev. **D32**, 189 (1985)
- 113 D. Ebert, R. Faustov, V. Galkin, Eur.Phys.J. **C66**, 197 (2010)
- 114 A. Parmar, B. Patel, P. Vinodkumar, Nucl.Phys. **A848**, 299 (2010)
- 115 N. Brambilla et al. (Quarkonium Working Group) (2004), hep-ph/0412158
- 116 E.J. Eichten, K. Lane, C. Quigg, Phys. Rev. Lett. **89**, 162002 (2002), hep-ph/0206018
- 117 P.P. D'Souza, M. Bhat, A.P. Monteiro, K.B. Vijaya Kumar (2017)
- 118 Bhaghyesh, K.B. Vijaya Kumar, Y.L. Ma, Int. J. Mod. Phys. **A27**, 1250011 (2012)
- 119 F. Giannuzzi, Phys. Rev. **D78**, 117501 (2008)
- 120 J.T. Lavery, S.F. Radford, W.W. Repko (2009), 0901.3917
- 121 C.R. Munz, Nucl. Phys. **A609**, 364 (1996)
- 122 C.S. Kim, T. Lee, G.L. Wang, Phys. Lett. **B606**, 323 (2005)
- 123 D. Ebert, R.N. Faustov, V.O. Galkin, Mod. Phys. Lett. **A18**, 601 (2003)
- 124 N.A. Tornqvist, Phys. Lett. **B590**, 209 (2004)
- 125 E. Braaten, M. Lu, Phys. Rev. **D76**, 094028 (2007)
- 126 M. Albaladejo, F.K. Guo, C. Hanhart, U.G. Meiner, J. Nieves, A. Nogga, Z. Yang, Chin. Phys. **C41**(12), 121001 (2017)
- 127 C. Hanhart, Yu.S. Kalashnikova, A.E. Kudryavtsev, A.V. Nefediev, Phys. Rev. **D76**, 034007 (2007)
- 128 C.W. Zhao, G. Li, X.H. Liu, F.L. Shao, Eur. Phys. J. **C73**, 2482 (2013)
- 129 X. Liu, Z.G. Luo, Z.F. Sun, Phys. Rev. Lett. **104**, 122001 (2010)
- 130 F.K. Guo, C. Hanhart, G. Li, U.G. Meissner, Q. Zhao, Phys. Rev. **D83**, 034013 (2011)
- 131 G. Li, Q. Zhao, Phys. Lett. **B670**, 55 (2008)
- 132 G. Li, Q. Zhao, Phys. Rev. **D84**, 074005 (2011)
- 133 S.S. Afonin, I.V. Pusenkov, EPJ Web Conf. **125**, 04006 (2016)